Biochemistry and Biophysics Reports 33 (2023) 101424

Contents lists available at ScienceDirect

Biochemistry and Biophysics Reports

journal homepage: www.elsevier.com/locate/bbrep

Molecular and phylogenetic analysis of a type K1 strain *Trypanosoma evansi* isolate from Nigerian cattle: An evaluation of the therapeutic effects of compounds from *Brassica oleracea* on the histopathology of infected wister rats

Kingsley Onyekachi Moh [a,*], Sodangi Abdulkarim Luka [b], Iliya Shehu Ndams [b], Idris Alao Lawal [c], Dahiru Sani [d], Sylvester Sunday Obeta [e], Gbenga Peter Oderinde [f], Emeka John Dingwoke [g], Fatima Amin Adamude [h], Abraham Ehinomhen Ubhenin [h], Saifullahi Umar [i]

[a] *Department of Biology, Faculty of Life Sciences, Ahmadu Bello University, Zaria, Kaduna State, Nigeria*
[b] *Department of Zoology, Faculty of Life Sciences, Ahmadu Bello University, Zaria, Kaduna State, Nigeria*
[c] *Department of Veterinary Parasitology and Entomology, Faculty of Veterinary Medicine, Ahmadu Bello University, Zaria, Kaduna State, Nigeria*
[d] *Department of Veterinary Pharmacology and Toxicology, Faculty of Veterinary Medicine, Ahmadu Bello University, Zaria, Kaduna State, Nigeria*
[e] *Department of Veterinary Parasitology and Entomology, Faculty of Veterinary Medicine, University of Abuja, Nigeria*
[f] *Department of Human Anatomy, Faculty of Basic Medical Sciences, Ahmadu Bello University, Zaria, Kaduna State, Nigeria*
[g] *UNESCO-International Center for Biotechnology, University of Nigeria, Nsukka, Enugu State, Nigeria*
[h] *Department of Biochemistry, Faculty of Medical Sciences, Federal University Lafia, Nasarawa State, Nigeria*
[i] *Department of Pharmacognosy and Drug Development, Faculty of Pharmaceutical Sciences, Bayero University Kano, Kano State, Nigeria*

ARTICLE INFO

Keywords:
K1 strain *Trypanosoma evansi*
Trypanosomiasis
Phylogenetics
Spacer-1 ribosomal RNA
Histopathology
Phenonic-rich compounds

ABSTRACT

Background: Understanding the pathogenesis of animal trypanosomiasis can be improved by studying the genetics of bovine trypanosomes. Pathogenic animal trypanosomes are a major impediment to livestock production, with negative economic consequences spreading beyond Sub-Saharan Africa to subtropical regions of Northern Africa, Southeast Asia, and Central and South America. An atypical K1 strain of *Trypanosoma evansi* (*T. evansi*) isolates from infected cattle in Nigeria was analyzed. The therapeutic effect of phenolic-rich compounds on the histopathology of wistar rats infected with the K1 strain was studied.

Methods: The K1 strain *T. evansi* was analyzed molecularly using PCR and sequence analysis of the Spacer-1 ribosomal RNA gene. To assess the evolutionary relationship, this was phylogenetically compared to other species studied in different parts of the world. Thirty adult male wistar rats were divided into six groups of five each. Animals in group A served as the standard control (not infected). Group B animals were infected but not treated. Group C animals were infected and given 3.5 mg/kg body weight of the standard drug diminazene aceturate. Animals in groups D, E, and F were infected and treated with phenolic-rich compounds isolated from *Brassica oleracea* (*B. oleracea*) at concentrations of 100, 200, and 400 mg/kg body weight, respectively. The phytochemicals were extracted using standard analytical procedures, and GCMS analysis revealed the presence of phenolic-rich compounds. The animals were given 0.2 mg/ml trypanosome intraperitoneally, diluted with normal saline. The vital organs of the animals were harvested and histologically examined.

Results: The nested PCR amplification of the trypanosome's ITS-1 region revealed a DNA amplicon of 627 base pairs. The rRNA nucleotide sequence was deposited in GenBank under the accession number MN462960. Basic Local Alignment search of the obtained ITS-1 rRNA sequences revealed that the K1 strain trypanosome and other strains from different regions have an evolutionary relationship. The phenolic-rich compounds had protective effects on the organs of infected animals, resulting in a decrease in parasitemia levels. They have anti-trypanosome activities at the minimum and maximum effective doses of 200 and 400 mg/kg body weight, respectively.

* Corresponding author. Department of Biology, Faculty of Life Sciences, Ahmadu Bello University, Zaria, Nigeria.
E-mail address: onyekachimoh@gmail.com (K.O. Moh).

https://doi.org/10.1016/j.bbrep.2023.101424
Received 23 June 2022; Received in revised form 4 January 2023; Accepted 5 January 2023

Conclusions: The K1 strain *T. evansi* was isolated from naturally infected cattle in this study. The results indicate that phenolic-rich compounds have anti trypanosoma activities capable of healing organ damage caused by trypanosomiasis.

1. Introduction

Trypanosomes are unicellular hemoflagellate protozoa belonging to the trypanosomatidae and trypanosoma families and genera, respectively. The genus *trypanosoma* contains several species, including *T. brucei*, *T. equiperdum*, and *T. evansi*, which cause trypanosomiasis. Surra is caused by *T. evansi* in domestic and wild animal reservoirs, as well as in humans [1–4]. The disease is still endemic in Sub-Saharan Africa [5–10], and it has historically prevented the development of vast swaths of African land into highly productive agricultural areas [9]. The disease has a significant socioeconomic impact and reduces animal productivity globally [11]. *T. evansi* has the broadest range of hosts and geographical distribution of any pathogenic trypanosoma species, infecting a wide variety of mammalian hosts and other animals [11,12], and causing wasting disease (*Surra*) in livestock [10,12]. *T. evansi* was the first pathogenic mammalian trypanosome discovered in the blood of Indian equines and dromedaries in 1880 by Dr. Griffith Evans [11,13]. Following the loss of its genetic material maxicircle kinetoplast DNA, *T. evansi* evolved from its ancestral *T. brucei* through mechanical transmission, allowing it to spread beyond the tsetse belt in Africa [11]. Anemia and infertility are common clinical manifestations of *T. evansi* infection. It is spread mechanically by hematophagous flies of the genera *Stomoxys* and *Tabanus* [10,11].

T. evansi has spread beyond its original Sub-Saharan Africa to subtropical regions of Northern Africa, Southeast Asia, and Central and South America due to the loss of its genetic material (kinetoplast DNA) and the inability to undergo cyclical transmission [14]. According to reports, the importation of infected dromedary camels from the Canary Islands caused *Surra* outbreaks in France [15] and Spain [16].

T. evansi has been reported to have zoonotic potential in India [17,18] and Vietnam [7]. *Surra* was thus classified as a notifiable multispecies animal disease by the World Organization for Animal Health (OIE) [19]. The *Surra* epidemic has been linked to a chronic failure in transboundary animal vaccination, which has serious implications for global trade in live animals and animal products [12]. There is currently no viable strategy for reducing trypanosomiasis transmission through the use of an effective anti-trypanosoma agent. As a result, control is still based on a combination of active case diagnosis and treatment, as well as vector control [20,21]. In the absence of effective vaccination, due to surface membrane modification [10], control of trypanosomiasis could be achieved primarily through chemoprophylactic or chemotherapeutic agents [22], so investigating other options became important.

Morphological and species concepts are important considerations in bovine trypanosomiasis, particularly because morphological differentiation of *T. brucei*, *T. equiperdum*, and *T. evansi* is difficult [8], especially since *T. brucei brucei* and *T. evansi* are morphologically identical [23]. This emphasizes the importance of genetically identifying trypanosomes of interest. *T. evansi* was identified in this study through a PCR-based approach, partial gene sequencing targeting its internal transcribed spacer-1 ribosomal RNA gene, and phylogeny.

The plant-based system is being used extensively in the search for effective and alternative chemotherapy and chemoprophylaxis as the mainstay for the control of animal trypanosomiasis. The plants contain a diverse range of unique and effective medicinal substances that can be used to treat a variety of disease conditions. *B. olercea* (L. var. capitata) is one of these plants. It is a member of the Cruciferae family, which includes broccoli, cauliflower, and kale [24]. According to research findings, the main constituents of *B. olercea* include carbohydrates, which account for approximately 90% of the dry weight, with approximately one-third being dietary fiber and two-thirds being low molecular weight carbohydrates.

Glucosinolates are another biological component of the plant [25]. *Brassica* species have been shown to have cancer-preventive properties [26], which have been linked to glucosinolates and their derivatives [27]. *B. oleracea* has become very useful in traditional medicine due to its medicinal value, which includes antioxidant, anti-inflammatory, antibacterial, and tumor-protective properties [28]. When included in many commercial weight-loss diets [29], the juice improves non-heme iron bioavailability [30] and can be used as an alternative therapy for cancer patients [31].

B. oleracea appears to have anti-trypanosoma activity. In a previous study, the aqueous extract was found to be effective in vitro anti-trypanosoma activity by immobilizing the trypanosomes within 3 h of incubation, rendering the parasites not infective to mice [32]. Similarly, a study that looked at the anti-trypanosoma and cytotoxicity effects of methanolic extracts of *B. oleracea* fruits and leaves against *T. evansi* on Vero cell lines grown in Dulbecco's Modified Eagle Medium with foetal calf serum reported a trypanocidal activity from immobilization, reduction to the mortality of the trypanosomes [33]. The aim of this study was to analyze an atypical K1 strain of *Trypanosoma evansi* (*T. evansi*) isolates from infected cattle in Nigeria and determine whether phenolic-rich compounds had any therapeutic effect on the histopathology of wister rats that had been exposed to the strain.

2. Materials and method

2.1. Trypanosoma evansi

T. evansi was obtained from the Nigerian Institute for Trypanosomiasis Research (NITR) in Kaduna, Nigeria. Prior to the experiments, the parasite was submitted for phylogenetic and molecular analyses. In February 2018, the isolates were obtained from infected cattle. The collection of blood and analyses on experimental animals were carried out in accordance with Ahmadu Bello University's Ethics guidelines. Two (2) ml of blood was collected at random from the jugular vein of infected animals in a heparinized Venosafe tube (Terumo, Leuven, Belgium). The buffy coat samples were confirmed by micro haematocrit centrifugation and cryopreserved as previously described [34]. The experimental rat received 100 μl of thawed buffy coat intraperitoneally. Parasitaemia was measured in 2 μl of tail blood using the Herbert and Lumsden matching method [35], first on day 3 post inculation and then on a daily basis. The rat was anesthetized and blood was collected in a heparin sample bottle by heart puncture at the peak of parasitemia (**about 108.4 cells ml^{-1}**) on the fifth post-infection day. It was used to subinocuate other experimental rats after being diluted in an equal volume of phosphate buffered saline glucose (PSG; 7.5 g/l Na2H-PO42H2O, 0.34 g/l NaH2 PO4H2O, 2.12 g/l NaCl, 10 g/l D-glucose, pH 8).

3. Molecular analysis

3.1. Extraction of T. evansi genomic DNA

The genomic DNA of the atypical K1 strain trypanosome was extracted using a kit (DNeasy Blood & Tissue Kit, QIAGEN Germany) as directed by the manufacturer. Nested Polymerase Chain Reaction (Nested PCR) and optimization, as well as nucleotide sequencing, were performed. Twenty (20) μl of proteinase K was pipetted into a 1.5 ml labeled microcentrifuge tube, followed by 100 μl of a blood sample containing the parasites. With Phosphate Buffer Saline, the mixture was

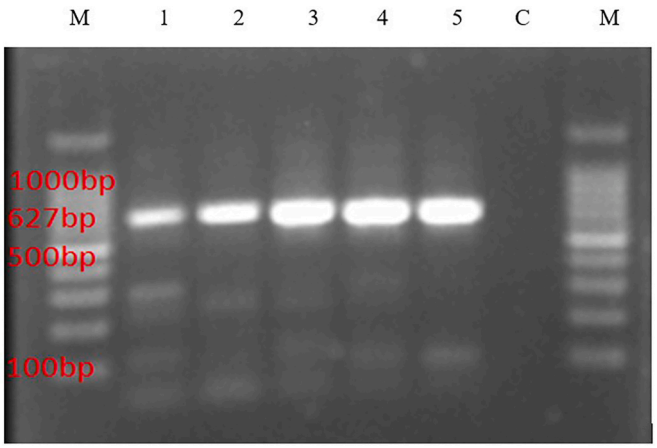

Fig. 1. PCR amplification of the K1 strain *T. evansi* DNA.
M: molecular marker (100bp); Lanes 1, 2, 3, 4 and 5: DNA sample; C: Control.

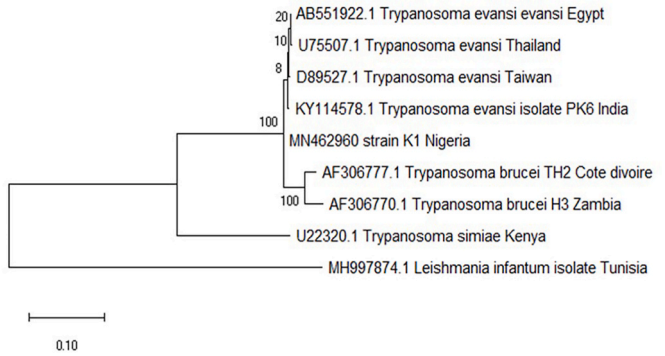

Fig. 2. Maximum likelihood phylogenetic tree illustrating the evolutionary relationship of T. *evansi* with other GenBank species used in this study.

made up to a total volume of 220 μl. To the blood sample, 200 μl lysis Buffer AL of 216 ml concentration (AL) was added and mixed thoroughly by vortexing. Then 200 μl ethanol (96–100%) was added and mixed thoroughly by vortexing. The mixture was then transferred into a DNeasy Mini spin column placed in a 2 ml collection tube and centrifuged at 6000×*g* (8000 rpm) for 1 min; the flow-through and the collection tube were discarded. The spin column was placed in a new 2 ml collection tube and 500 μl Buffer AW1 of 242 ml (AWI) concentration added to the mixture and centrifuged for 1 min at (8000 rpm). The flow-through and the collection tube was also discarded. The washing process was repeated by adding 500 μl Buffer AW2 of 342 ml concentration (AW2) and centrifuged for 3 min at 20,000×*g* (14,000 rpm), the flow-through and collection tube was discarded. The spin-column was then transferred into a new 1.5 centrifuge tube and the DNA was eluted by adding 200 μl Buffer AE at the center of the spin column membrane. This was incubated for 1 min at 26 °C, and centrifuged for 1 min at 8000 rpm. Determination of DNA concentration was done using Nanodrop® ND 1000 Spectrophotometer according to the manufacturer's protocols and was recorded at 260/280 wavelength. The DNA was stored at −20 °C prior to the Nested Polymerase Chain Reaction assay.

3.2. Primer design

A set of primer 5′–3′ (ITS1- outer forward: TGCAATTATTGGTCGCGC) (ITS1- outer reverse: CTTTGCTGCGTTCTT) (ITS1- inner forward: TAGAGGAAGCAAAAG) (ITS1- inner reverse: AAGCCAAGTCATCCATCG) was provided for nested PCR targeting the Internal Transcribed Spacer 1 (ITS-1) region of the trypanosome ribosomal DNA, which separates 18S from 5.8S RNA [34].

3.3. Nested PCR

Nested PCR was used to separate 18S from 5.8S RNA by targeting the Internal Transcribed Spacer 1 (ITS1) region of trypanosome ribosomal RNA [36]. The nested PCR used ITS-1 primer for generic and specific identification of K1 strain *T. evansi* with an expected amplicon of 430 bp [37]. It was carried out in a 25 μl reaction containing 1 ng/μl of DNA template, 2 μl of 10 × PCR buffer, 1.0 μl of 25 mM $MgCl_2$, 1.0 μl of 5 pMol forward primer, 1.0 μl of 5 pMol reverse primer, 1.0 μl of DMSO, 2.0 μl of 2.5 Mm DNTPs, 0.1 μl of Taq DNA polymerase 5 U/μl, and 13.4 μl of nuclease-free water (Sigma-Aldrich). The tubes were then placed in a programed Applied Biosystems Veriti 96 well Thermocycler (Germany). Cycling conditions were as follows: initial denaturation at 94 °C for 5 min, 9 cycles of denaturation at 94 °C for 15 s, annealing temperature of 65 °C for 20 s, extension at 72 °C for 30 s, final extension at 72 °C for 7 min, and hold a temperature of 10 °C. In the second reaction, 0.5 μl of the first round reaction's PCR product was mixed with 25 μl of the second round reaction in a new PCR tube. The cycling conditions for nested PCR were the same.

3.4. Electrophoresis and purification of the PCR products

Electrophoresis on 1.5% Agarose gel with an aliquot of 4 μl of the PCR products and 100 bp of DNA ladder stained with SYBR Green for 1 h at 80 V was used to analyze the amplified products. Following the manufacturer's protocol, the PCR products were purified using MegaExtractor-PCR and Gel Clean-up. The PCR amplicons were electrophoresed to determine the size of the amplified fragments by comparing them to a standard molecular weight marker (100 bp DNA ladder). The PCR products were analyzed using a 1.5% agarose gel, which was prepared by weighing 1.5g of agarose powder, pouring it into a conical flask containing 1 × TAE buffer, and heating it in a microwave oven until completely dissolved. This was taken out of the oven and allowed to cool. SYBR Green staining dye (Roche Diagnostic, Mannheim, Germany) was added and thoroughly mixed. Before pouring the gel, the ends of the trays were sealed with masking tape and the combs were inserted to ensure that no bubbles formed. The masking tapes and combs were carefully removed from the gel casting tray. After placing the tray in the electrophoresis tank, 1 × TAE buffer was added to cover the gel. The molecular weight marker was loaded into the first and last wells, the control (nuclease-free water) was loaded into the second well, and the samples were loaded into the subsequent wells. Before turning on the power pack to run the gel for 30 min at 80 V, the safety cover was placed. The gel was removed and placed in the transilluminator and documentation system for the gel image to be captured. The DNA template-containing agarose block was cut into small pieces and placed in 1.5 ml microtubes. 400 μl of the binding solution was added and incubated at room temperature, vortexed every 2–3 min until the gel pieces were completely dissolved. Thirty (30) μl magnetic beads were added and vortexed every 10 s for 2 min before placing each tube in the magnetic stand until the magnetic beads were completely separated from the specimen solution. Following the magnetic capture, the supernatant was carefully removed. The beads were immersed in 600 μl of washing solution, which was vortexed for 10 s. The magnetic stand was used to hold each tube. The magnet was used to collect the beads, and the supernatant was carefully removed after the magnetic capture. The tube was vortexed after one (1) ml of 75% ethanol was added. After flash centrifugation, this was repeated until the ethanol was completely removed. After 10 s, 25 μl of sterilized water was added and mixed. After a brief vortexing, the solution was incubated at room temperature for 2 min before being placed in the magnetic stand. The supernatant was collected and transferred to a new tube.

3.5. Sequencing and analysis of sequences

The PCR products were sequenced directly using Big Dye Terminator

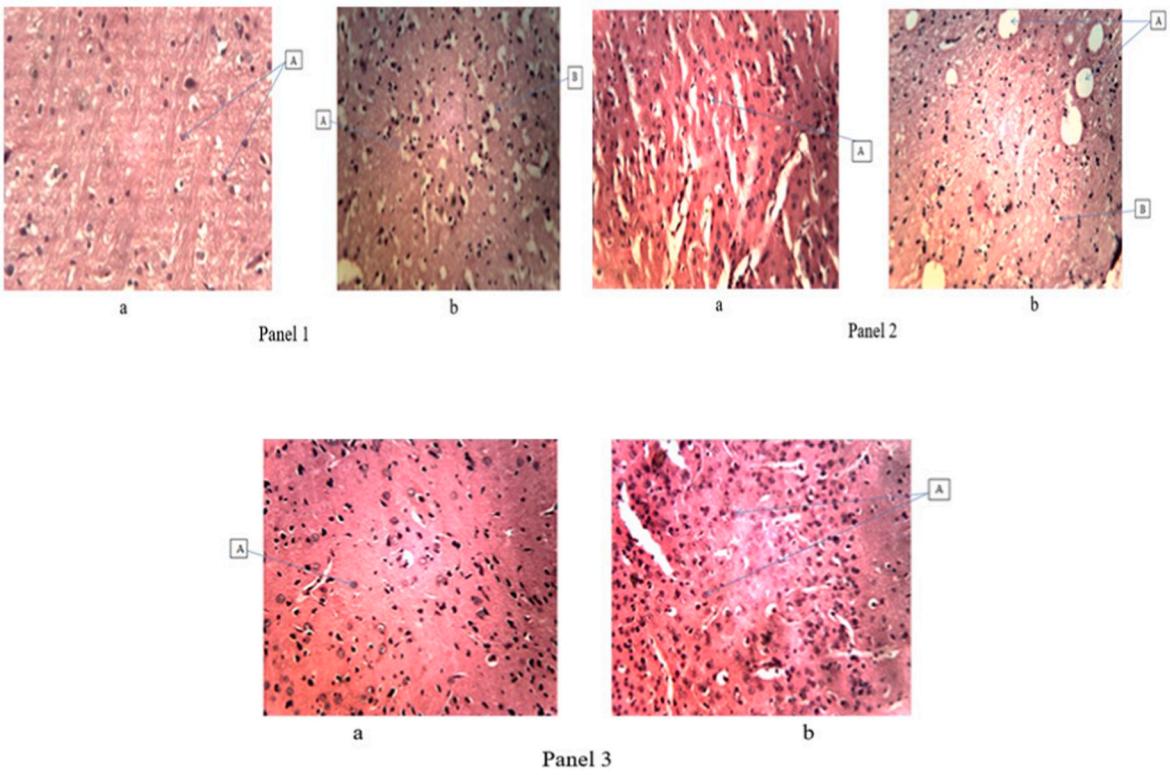

Fig. 3. Brain histology photomicrograph (H&E, 40 ×)
Panel 1: (a) Brain of rat uninfected/untreated showing normal neurons (A); (b) Brain of rat infected/untreated showing vacoulation (A) and necrosis (B). **Panel 2**: (a) brain of the *T. evansi* infected rat and treated with 3.5 mg/kg body weight diminazene aceturate showing necrosis (A); (b) brain of rat infected/treated with 100mg/kg body weight phenolic-rich compounds of *B. oleracea* showing fat droplets (A) and vacuolation. **Panel 3**: (a) brain of rat infected/treated with 200mg/kg body weight of the compounds showing normal nervous tissues (A); (b) brain of rat infected/treated with 400mg/kg body weight of the compounds showing normal neurons (A).

v3.1 Cycle Sequencing Kit (Applied Biosystems, Foster City, CA, USA), with the forward amplification PCR primers and AmpliTaq-FS DNA Polymerase. MEGA X was used to edit the chromatographs for the sequences in order to obtain consensus sequences. The obtained forward and reverse sequences were trimmed and edited using BioEdit software before being aligned to produce a single sequence product for the DNA products. Each sequence was imported into the NCBI Database and compared to other sequences in the GenBank using the Nucleotide Basic Local Alignment Tool (BLAST).

3.6. Submission of nucleotide sequence to the GenBank

The nucleotide sequence of the *T. evansi* ITS-1 ribosomal RNA gene used in this study was submitted to GenBank (http://www.ncbi.nlm.nih.gov/genbank/) and an accession number was obtained.

3.7. Phylogenetic analysis

The phylogenetic analysis [38] of the K1 strain trypanosome used in this study was performed using the Molecular Evolutionary Genetics Analysis (MEGA X) software program. A computer Notepad page was opened, and the sequences were saved in FASTA format. Other *trypanosoma* species' sequences and some genetically distant isolates were obtained from GenBank and pasted onto the Notepad page. Multiple alignments of all the sequences were performed using Clustal W for pairwise comparison. MEGA 7.0 software was used to manually edit and annotate the aligned sequences. To construct the phylogenetic tree, the genetic distances between pairs of sequences were calculated using the Maximum Likelihood method algorithm in the Tamura-Nei model [39].

3.8. Plant material

Fresh *B. oleracea* leaves were obtained from a local market in Samaru, Zaria, Kaduna State, Nigeria. A taxonomist at Ahmadu Bello University's Department of Botany's Herbarium in Zaria, Nigeria, authenticated the leaves. For reference, voucher number 43809 was deposited.

3.9. Extraction of phenolic-rich compounds from B. oleracea leaves

The leaves were thoroughly washed with tap water and air-dried at room temperature in the shade. Using a mortar and pestle, the leaves were ground into powder. At room temperature, 500g of pulverized leaves were extracted by cold maceration with 500 ml of 80% petroleum ether. The petroleum ether portion was concentrated and labeled at room temperature. The defatted marc was exhaustively extracted with methanol at room temperature, and the combined methanol extract was partitioned with ether:water 1:1. The water portion was partitioned once more with n-butanol. The butanol portion was collected, partitioned with 1% potassium hydroxide, and concentrated at room temperature to yield the saponin fraction, which was labeled appropriately. The potassium hydroxide portion was partitioned again with 2% hydrochloric acid:butanol 1:1. The butanol portion was then collected in a porcelain dish and concentrated at room temperature using sterile Whatman filter paper 1. Under standard analytical conditions, an aliquot of this extract was analyzed using GCMS-QP 2010 plus Shimadzu, Japan. The compounds were identified using the Mass Spectral Library (NIST/EPA/NIH 11, version 2.0).

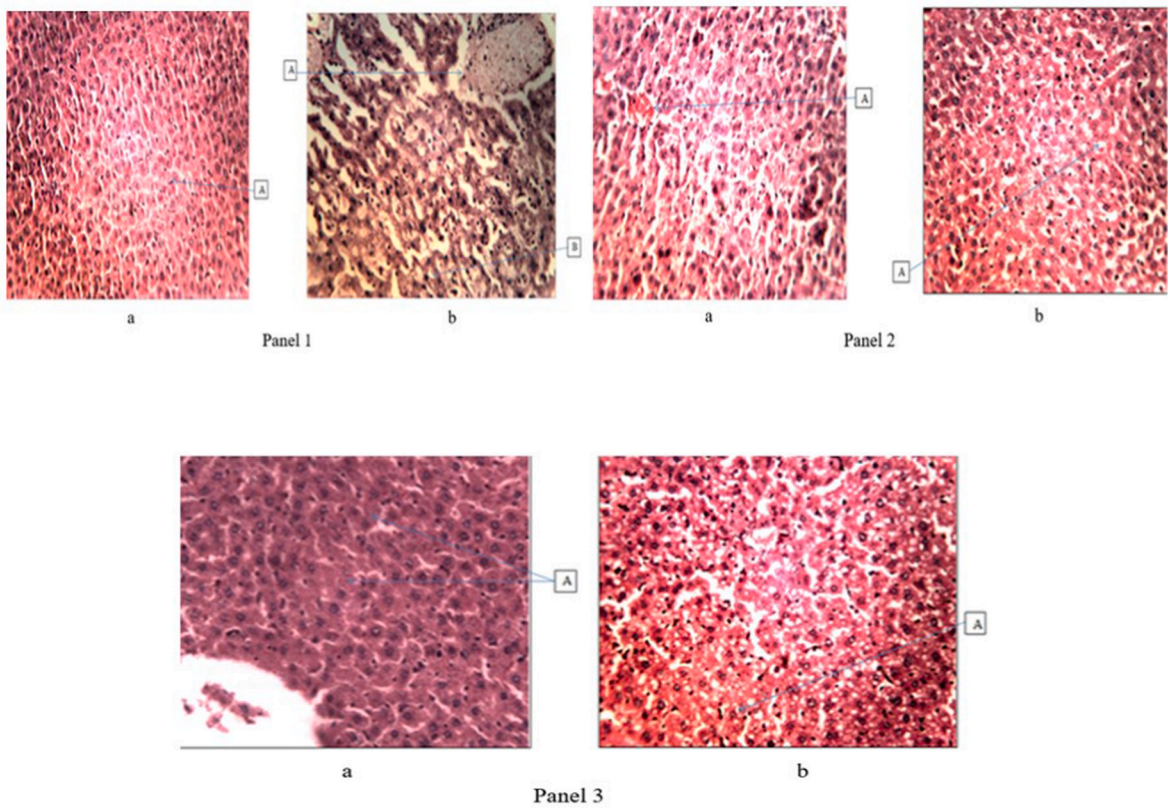

Fig. 4. Liver histology photomicrograph (H&E, 40 ×)
Panel 1: (a) Liver of rat uninfected/untreated showing normal kupfer Cell (A); (b) Liver of rat infected/untreated showing vascular congestion (A) and necrosis (B). **Panel 2**: (a) Liver of rat infected/treated with 3.5 mg/kg body weight diminazene aceturate showing vascular congestion (A); (b) Liver of rat infected/treated with 100mg/kg body weight phenolic-rich compounds of *B. oleracea* showing necrosis (A). **Panel 3**: (a) Liver of rat infected/treated with 200mg/kg body weight of the compounds of showing normal hepatocytes (A); (b) Liver of rat infected/treated with 400mg/kg body weight of the compounds showing cytoplasmic vacuolation (A).

3.10. Experimental design

Prior to the experiments, the Ahmadu Bello University Committee on Animal Use and Care (ABUCAUC) granted ethical approval with the approval number ABUCAUC/2018/003. The animals were handled in accordance with internationally recognized standards for animal welfare. The University's Committee on Animal Use and Care established guidelines for animal care and treatment, which were followed. The animals were housed in a netted animal house at Ahmadu Bello University, Faculty of Veterinary Medicine, Department of Veterinary Parasitology and Entomology. They were allowed to acclimate for two weeks before being fed grower mash and water as needed. During the acclimatization period, the animals' baseline data were collected. The acute toxicity test was performed on thirteen laboratory animals weighing between 150 and 160g using Lorke's 1983 method. Thirty animals aged 6–7 weeks were divided into six groups of five animals each: A, B, C, D, E, and F. Group A animals were not infected and served as the negative control. Group B animals were infected but not treated, serving as the positive control. Group C animals were infected and treated with 3.5 mg/kg body weight of diminazene aceturate as the standard control. Animals in groups D, E, and F were all infected and treated with phenolic-rich compounds at doses of 100, 200, and 400 mg/kg body weight, respectively.

3.11. Acute toxicity test

The acute toxicity test was conducted in two stages [40]. First, the mice were divided into four groups of three. In this case, one group served as the control, while the other three served as the test groups. The mice in the control group were given 1 ml of normal saline via oral gavage, while the mice in the test groups were given extract concentrations of 10, 100, and 1000 mg/kg body weights. The extract doses were chosen in accordance with the guidelines established by the Organization for Economic Cooperation and Development (OECD) for the testing chemicals.

All administrations were made in the form of a single oral dose. At 1, 2, 4, 8, 12, 24, 48, and 72 h, the mice were examined for signs of toxicity and mortality. At this stage, the behavior, respiratory pattern, cardiovascular symptoms, motor activity, reflex, and fur and skin changes were all considered. The second stage of the experiment began because there was no mortality at the intervals. At this point, the mice were divided into four groups of three mice each (one control group and three test groups). The mice in the three test groups were given extract doses of 1600, 2900, and 5000 mg/kg body weights, respectively. The mice were then examined again for toxicity signs and mortality.

3.12. Histopathological examination

On the final day of the experiment, the animals were sacrificed for histopathological analysis. The animals' brains, kidneys, livers, spleens, hearts, and testicles were removed and immediately placed in 10% formalin. The tissues were dehydrated in 70, 80, 95, and 100% alcohol for 1 h before being transferred to xylene and allowed to stand for 3 h. Following that, the tissues were placed in paraffin wax and impregnated for 4 h at 35 °C using an automated tissue processor (Sakura, Japan). Using a wax dispenser, paraffin wax was poured into an iron pan covered with an embedding ring and allowed to solidify. For decolorizing, 1% acid alcohol was placed in clean tap water and left for 45 min. The tissues were then immersed in eosin for 2 min before being rinsed with clean tap water and placed in 70, 80, 95%, absolute alcohol, and finally

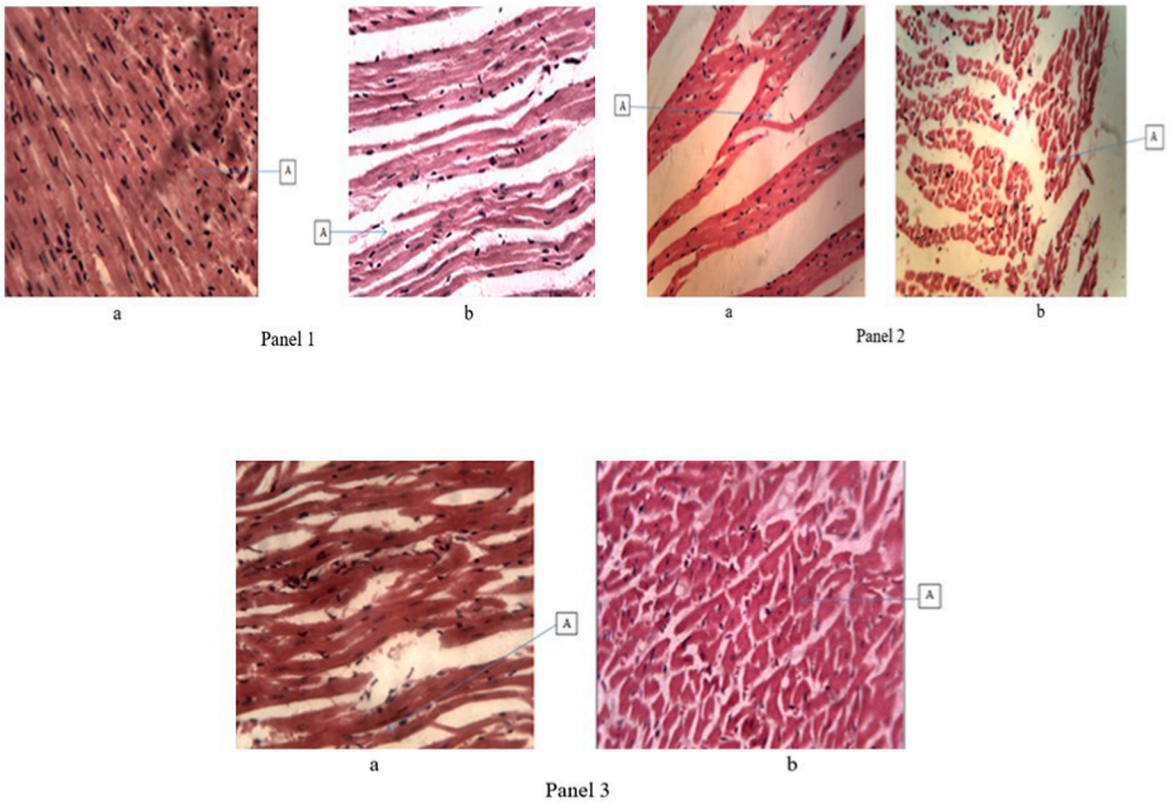

Fig. 5. Heart histology photomicrograph (H&E, 40 ×)
Panel 1: (a) Heart of rat uninfected/untreated showing normal cardiac muscle (A); (b) Heart of rat infected/untreated showing separation of fibers (A). **Panel 2**: (a) Heart of rat infected/treated with 3.5 mg/kg body weight diminazene aceturate showing loss of striation of cardiac muscle (A); (b) Heart of rat infected/treated with 100 mg/kg body weight phenolic-rich compounds of *B. oleracea* showing loss of striation of cardiac muscle (A). **Panel 3**: (a) Heart of rat infected/treated with 200mg/kg body weight of the compounds showing separation of fibers (A); (b) Heart of rat infected/treated with 400mg/kg body weight phenolic-rich compounds of *Brassica oleracea* showing normal cardiac muscle (A).

xylene. Serial sections of 5 mm thickness were cut using a microtome (**Model RM2245**, Leica Biosystems, Wetzlar, Germany) and stained with hematoxylin, eosin was made and mounted on sterile glass slides, and light microscopy was used to examine them [41].

3.13. Statistical analysis

FinchTV software version 1.4.0 was used to edit *T. evansi* sequences. Multiple alignments of all sequences were performed in MEGA X software version 10.0.5 using Clustal W for pairwise comparisons. The phylogenetic tree was built using the Maximum Likelihood algorithm [39]. MEGA X software version 10.0.5 was used to evaluate the branching of the phylogenetic tree using a bootstrap of 100 replicates [38].

4. Results

4.1. Nested PCR

The Nigerian *T. evansi* atypical strain from naturally infected cattle is known as the K1 strain. The nested PCR amplification of the ITS-1 region revealed that all of the DNA samples had the same 627 base pair amplicon (Fig. 1). The nucleotide sequence was submitted to GenBank under the accession number MN462960.

4.2. Phylogenetic analysis

The trypanosome shares similarities with *T. evansi* from Egypt, Thailand, Taiwan, and India, and is distantly related to *T. simiae* from Kenya, *T. brucei* TH2 from Cote divoire, and *T. brucei* H3 from Zambia, according to phylogenetic analysis (Fig. 2). They were also discovered to be distantly related to a Tunisian isolate of *Leishmania infantum*.

4.3. Histological analysis

Treatments with 200 and 400 mg/kg body weights of the phenolic-rich compounds protected brain tissues from histopathological damage and resulted in a significant decrease in parasitemia across all infected rats. There was no liver damage in animals given 400 mg/kg body weight of phenolic-rich compounds. The animals' heart and kidney tissues were protected when they were given 400 mg/kg body weight of the compounds. Except for the treatment with 100 mg/kg body weight, various tissue damages were observed in the spleens of the groups treated with 200 and 400 mg/kg body weights of the compounds. The testes in all treatment groups had no histopathological damage. Interestingly, the compounds derived from other plants in the same family were used to treat the infected rats; however, they had no discernible therapeutic effect. This suggests that the observed effect is plant-specific rather than the result of the phenolic-rich compounds' purification process. The phenolic compounds identified by gas chromatography and mass spectrometry (GCMS) analysis include phenol, 3,5–206 bis(1,1-dimethylethyl), 1-Hexadecene, Octane, 2,4,6-trimethyl, Cyclohexane, decyl, and cyclohexane. Undecyl, 5-eicosene, cyclohexane 1,2-Benzenedicarboxylic acid, bis(2-methylpropyl) ester, phthalic acid, butyl 336 ester, butyl glycolate ester n-Hexadecanoic acid, Eicosane, 7,9-Di-tert-butyl-1276-oxaspiro(4,5)deca-6,9-diene-2,8-dione, n-Pentadecylcyclohexane, 1-Heptacosanol, Hexanedioic acid, dioctyl ester, Undecane Cyclotetracosane, Octacosane, Cyclohexane, eicosyl, dl-2-Ethylhexyl

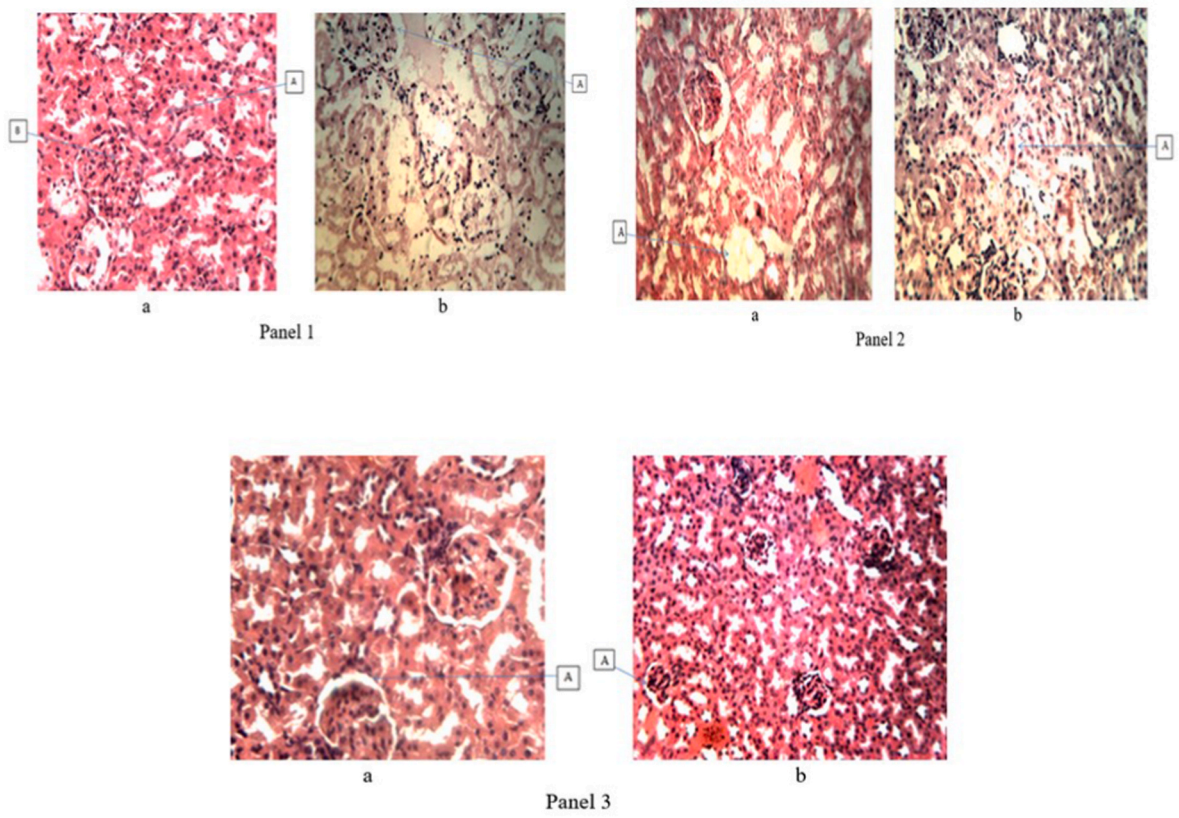

Fig. 6. Kidney histology photomicrograph (H&E, 40 ×)
Panel 1: (a) Kidney of rat uninfected/untreated showing normal tubules (A) and glomerulus (B); (b) Kidney of rat infected/untreated showing increased Bowman's capsule space (A). **Panel 2**: (a) Kidney of rat infected/treated with 3.5 mg/kg body weight diminazene aceturate showing glomerular necrosis (A); (b) Kidney of rat infected/treated with 100mg/kg body weight phenolic-rich compounds of *B. oleracea* showing tubular necrosis (A) **Panel 3**: (a) Kidney of rat infected/treated with 200mg/kg body weight of the compounds showing normal Bowman's capsule (A); (b) Kidney of rat infected/treated with 400mg/kg body weight of the compounds of showing normal glomerulus (A).

chloroformate, 1-Octanol, 2-butyl, Tetratriacontane, and Dodecane, 2-cyclohexyl.

5. Discussion

The study discovered atypical strain of Nigerian *T. evansi* strain from naturally infected cattle, dubbed the K1 strain. A limitation of this study is the lack of use of maxicircle and minicircle PCRs to identify the current K1 isolates. The nucleotide sequence has been deposited in GenBank under the accession number MN462960. The nested PCR amplification of the ITS-1 region revealed that the sampled DNAs have the same amplicon of 627 base pairs. In a similar study, *T. evansi* from Tanzania was found to have a band size of 430 base pairs. The observed difference could be attributed to species variations. The current Nigerian K1 strain shared a high degree of similarity with *T. evansi* from Egypt, Thailand, Taiwan, and India. It differed significantly from *T. simiae* from Kenya, *T. brucei* TH2 from Cote divoire, and *T. brucei* H3 from Zambia. They are all linked to a *Leishmania infantum* isolate from Tunisia that was used as an out group. This is most likely due to the fact that trypanosomes and *L. infantum* are both members of the *trypanosomatidae* family [42]. The evolutionary relationship between *T. brucei* and *T. evansi* is attributed to the deletion of the maxicircle kinetoplastic DNA, which is the genetic material required for cyclical development in tsetse flies [11]. The phylogenetic analysis revealed that the K1 strain shares similarities with *T. evansi* from Egypt, Thailand, Taiwan, and India, confirming the distribution of trypanosomes beyond the African continent [12].

In this study, no histopathological changes were observed in the organs of all uninfected animals. The various tissue damages observed in the brain, liver, heart, kidney, spleen, and testis of infected and untreated animals could be attributed to parasite vascular degeneration [43]. This is consistent with the findings of previous studies, which found vascular degeneration in the liver, tubular degeneration in the kidney, and mild degenerative changes in the brain of Swiss albino mice infected with *T. evansi* [44–46]. The histopathological damage in the brain of the animals infected and treated with 100 mg/kg body weight of the compounds (Fig. 3) could be attributed to the parasites crossing the blood-brain barrier, causing the observed injuries to the brain tissue, either as a result of constant irritation caused by the parasites' presence or by the toxins released [44]. This research backs up previous findings that both *T. brucei brucei* and *T. brucei rhodesiense* bloodstream forms gained access to the brain parenchyma of mice within hours of infection, before a significant level of microvascular inflammation was detectable [47].

Normal brain features in infected animals treated with 200 and 400 mg/kg body weights of phenolic-rich compounds (Fig. 3, panel 3a and b) could be due to the compounds' therapeutic effect in eliminating parasites from the blood stream, resulting in the observed protection from tissue damage. A similar study [48] found normal neurons and neutrophils in the brains of *T. brucei*-infected Wistar rats treated with 200 mg/kg body weight *Moringa oleifera* methanolic leaf extract. The therapeutic efficacy of the phenolic-rich compounds was demonstrated at a dose of 400 mg/kg body weight, which protected the animals' heart tissues from damage and resulted in a decrease in parasitemia (results now shown). This was evident in the normal features observed in the hearts of animals infected and treated with 400 mg/kg body weight of

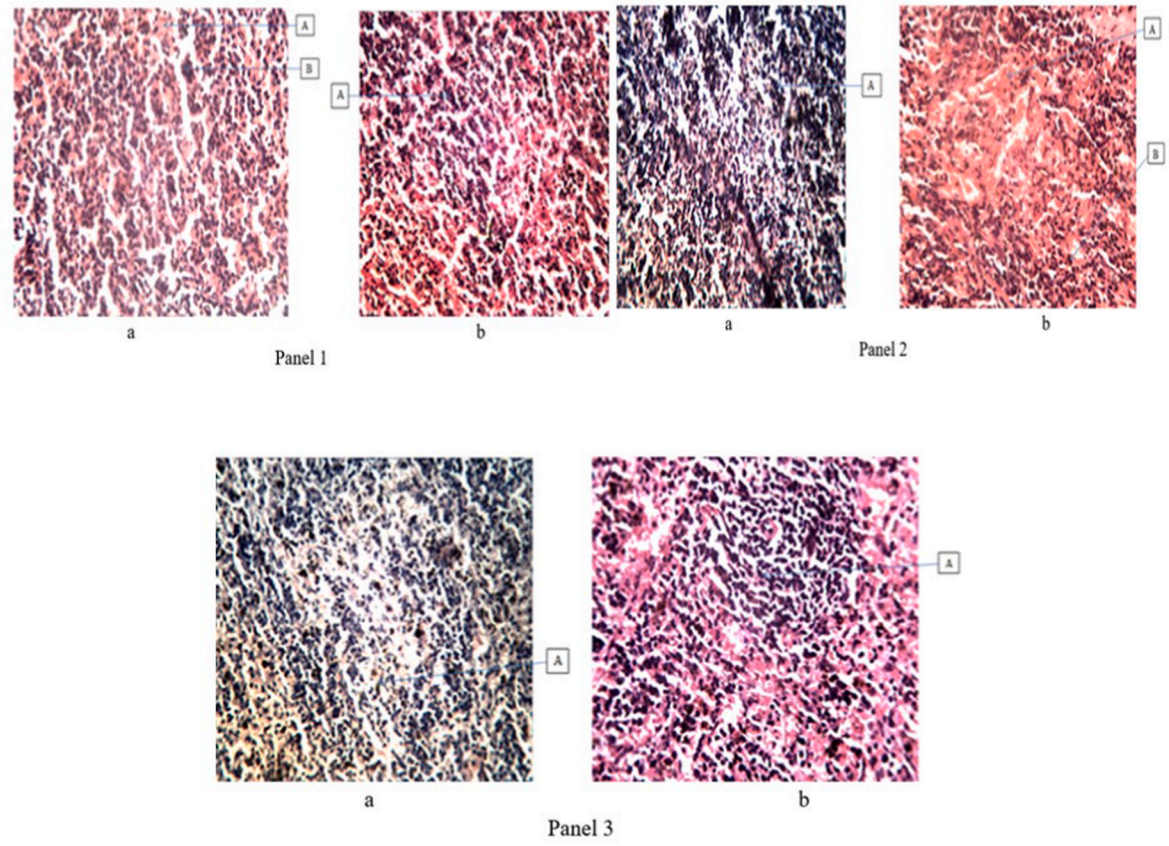

Fig. 7. Spleen histology photomicrograph (H&E, 40 ×)
Panel 1: (a) Spleen of rat uninfected/untreated showing normal red pulp (A) and white pulp (B); (b) Spleen of rat infected/untreated showing lymphocyte hyperplasia (A). **Panel 2**: (a) Spleen of rat infected/treated with 3.5 mg/kg body weight diminazene aceturate showing normal lymphocyte (A); (b) Spleen of rat infected/treated with 100 mg/kg bod weight phenolic-rich compounds of *B. oleracea* showing normal red pulp (A) and white pulp (B) distribution. **Panel 3**: (a) Spleen of rat infected/treated with 200mg/kg body weight of the compounds showing lymphocyte hyperplasia (A); (b) Spleen of rat infected/treated with 400mg/kg body weight of the compounds showing lymphocyte hyperplasia (A). (For interpretation of the references to color in this figure legend, the reader is referred to the Web version of this article.)

the compounds (Fig. 5, panel 3b), implying that the phytochemicals were trypanocidal or rendered the parasites immobile. Cardiovascular disease is one of the clinical signs of *T. evansi* trypanosomiasis [49]. The histopathological changes observed in the hearts of rats infected with parasites and treated with 100 mg/kg body weight of the compounds could be attributed to the parasites' overwhelming presence. This is demonstrated by the loss of cardiac muscle striation observed in the heart tissue (Fig. 5, panel 2b). The tubular necrosis in the kidneys of infected animals treated with 100 mg/kg body weight of the compounds (Fig. 6, panel 2b) indicated that a dose of 100 mg/kg body weight of the compounds was ineffective. It has been reported that the toxins released by trypanosomes may impair kidney function [46]. However, at 200 and 400 mg/kg body weights, the compounds protected the kidney from tissue damage, as evidenced by normal Bowman's capsule and glomerulus in the organs (Fig. 6, panel 3a and b). Splenomegaly, one of the clinical signs of trypanosomiasis, could explain the lymphocyte hyperplasia observed in the spleens of infected and untreated rats. The routine drug Diminazene aceturate was found to protect only the spleen (Fig. 7, panel 2a) and testis (Fig. 8, panel 2a) from tissue damage, but despite parasite clearance from the blood, diminazene aceturate could not protect the brain (Fig. 3, panel 2b), liver (Fig. 4 panel 2a), heart (Fig. 5, panel 2a), and kidney (Fig. 6, panel 2a) from tissue damage, resulting in lesions on their tissues. This reveals the efficacy limitations of Diminazene aceturate as well as the side effects [50]. The compounds were able to protect the spleen (Fig. 7) from tissue damage at a dose of 100 mg/kg body weight, indicating that this was an adequate and effective dose that produced the desired effect. This was seen in their tissues' normal red pulp and white pulp distributions (Fig. 7, panel 2b). The various histopathological damages observed in the spleens of animals treated with 200 and 400 mg/kg body weights phenolic-rich compounds, such as lymphocyte hyperplasia (Fig. 7, panel 3), suggest that the compounds could not protect the spleen from tissue injury and that the phytochemicals were ineffective at those doses. This is consistent with the discovery of apoptosis and white foci of varying sizes in the white and red pulps of mice infected with *T. congolense* and treated with a supernatant stem bark extract of *Commiphora swynnertonii* at 1500 mg/kg body weight [51]. The necrosis seen in the livers of animals given 100 mg/kg body weight demonstrated that the compounds could not protect the liver from tissue damage at that dose (Fig. 4, panel 2b). The presence of cytoplasmic vacuolation and necrosis in the livers of animals given 400 mg/kg body weight of the compounds suggested that, while the phytochemical was trypanocidal at that concentration, it lacked restorative activity (Fig. 4). The presence of normal hepatocytes in the livers of animals infected with parasites and treated with 200 mg/kg body weight of the compounds could be due to the parasites being eliminated from the rats' blood at a lower dose that did not harm the liver tissue. This suggests that phenolic-rich compound treatment at 200 mg/kg body weight protected the liver from damage. One of the clinical signs of trypanosomiasis was the necrosis of primary spermatogenic cells in the testis of infected and untreated rats (Fig. 8, panel 1b). This includes testicular degeneration in male animals, which results in the production of low-quality spermatozoa [52]. At all treatment doses, the

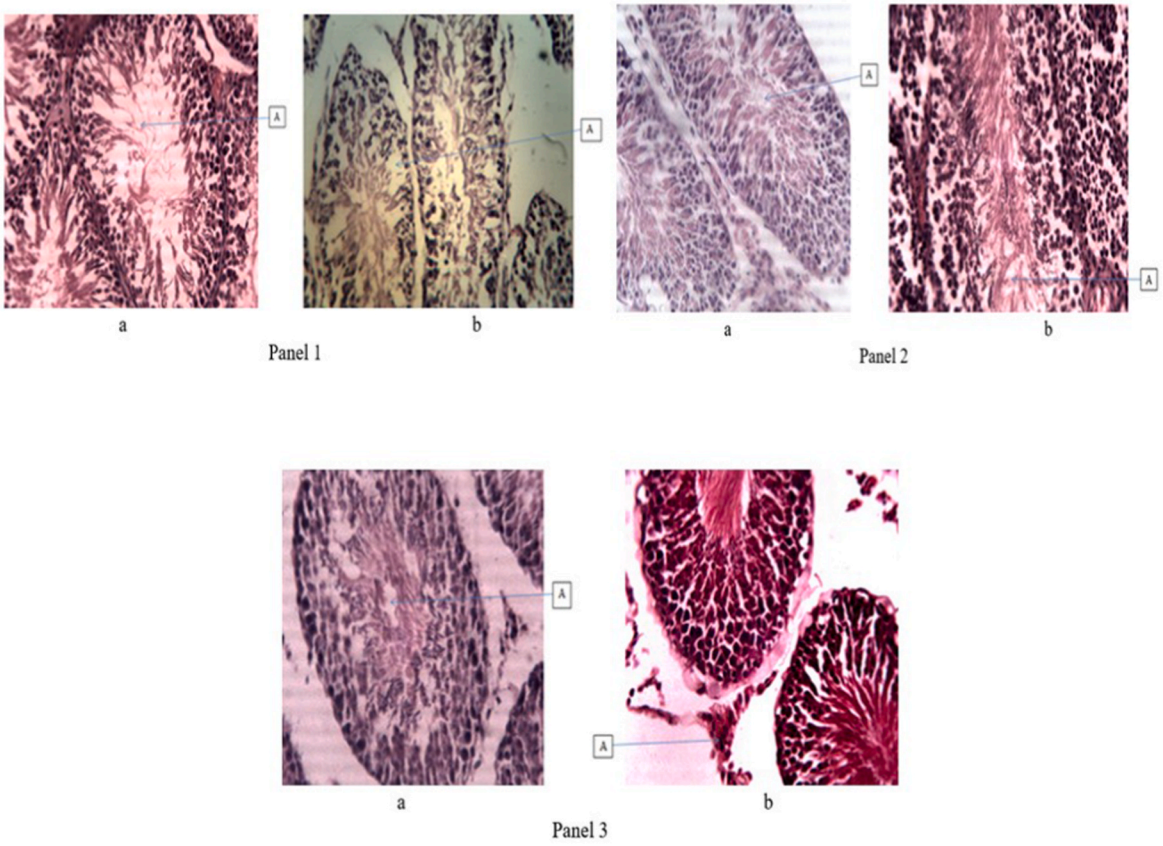

Fig. 8. Testis histology photomicrograph (H&E, 40 ×)
Panel 1: (a) Testis of rat uninfected/untreated showing normal seminiferous tubules (A); (b) Testis of rat infected/untreated showing necrosis of primary spermatogenic cells (A). **Panel 2**: (a) Testis of rat infected/treated with 3.5 mg/kg body weight diminazene aceturate showing normal seminiferous tubules (A); (b) Testis of rat infected/treated with 100mg/kg body weight phenolic-rich compounds of *B. oleracea* showing normal seminiferous tubules (A). **Panel 3**: (a) Testis of rat infected/treated with 200mg/kg body weight of the compounds of showing normal seminiferous tubules (A); (b) Testis of rat infected/treated with 400mg/kg body weight of the compounds showing normal epididymis (A).

phenolic-rich compounds were able to protect the testis from tissue damage. This was demonstrated by normal seminiferous tubules in the testis of animals treated with 100 mg/kg (Fig. 8, panel 2b) and 200 mg/kg (Fig. 8, panel 3a) body weights of the compounds, as well as normal epididymis in the testis of animals treated with 400 mg/kg (Fig. 8, panel 3b) body weight of the compounds. Diminazene aceturate, on the other hand, protected the testis from tissue damage, as evidenced by the presence of normal seminiferous tubules in the tissue. This could be attributed to the parasites being completely eliminated from the blood, resulting in no parasite attack on the tissue.

6. Conclusion

For the first time, an atypical K1 strain of *T. evansi* was isolated from naturally infected cattle in this study. The rRNA was sequenced and is now available in the Gene Bank under the accession number MN462960. Phylogenetic analysis revealed evolutionary relationships between the species and others studied in different parts of the world. The inclusion of phenolic-rich compounds from *B. oleracea* could aid in the development of effective trypanocides capable of repairing damaged organs after infection with *T. evansi*.

Authors' contributions

Sodangi Abdulkarim Luka, Iliya Shehu Ndams, Idris Alao Lawal, and Dahiru San supervised the work. All authors contributed equally in data collection and analysis. The manuscript was written by Kingsley Onyekachi Moh, Fatima Amin Adamude, and Emeka John Dingwoke. The authors read and approved the final manuscript.

Funding

This research received no external funding.

Availability of data and materials

Additional information will be provided upon reasonable request.

Ethics approval and consent to participate

This project was approved by the Ahmadu Bello University ethical committee on experimental animals.

Consent for publication

The authors declare their consent for publication.

Declaration of competing interest

The authors declare no conflict of interest.

Data availability

Data will be made available on request.

References

[1] H.M. Herrera, L.P.C. Aquino, R.F. TandMenezes, Trypanosoma evansi experimental infection in the South American coati (Nasunanasua); Hematological, biochemical and histopathological changes, Acta Trop. 81 (2002) 203–210.

[2] H. Mekata, S. Konnai, C.N. Mingala, N.S. Abes, C.A. Gutierrez, A.P. Dargantes, et al., Isolation, cloning, and pathologic analysis of Trypanosoma evansi field isolates, Parasitol. Res. 112 (2013) 1513–1521.

[3] M.R. Rjeibi, T.B. Hamida, Z. Dalgatova, T. Mahjoub, A. Rejeb, M. Dridi, M. Gharbi, First report of Surra (Trypanosoma evansi infection) in a Tunisian dog, Parasite 22 (2015) 3.

[4] P.P. Joshi, V.R. Shegokar, R.M. Powar, S. Herder, R. Katti, H.R. Salkar, V.S. Dani, A. Bhargava, J. Jannin, P. Truc, P, Human trypanosomiasis caused by Trypanosoma evansi in India: the first case report, Am. J. Trop. Med. Hyg. 73 (2005) 491–495.

[5] F.M. Haridy, M.T. El-Metwally, H.H. Khalil, T.A. Morsy, Trypanosoma evansi in dromedary camel: with a case report of zoonosis in greater Cairo, Egypt, J. Egypt. Soc. Parasitol. 41 (2011) 65–76.

[6] P. Truc, P. Buscher, G. Cuny, M.I. Gonzatti, J. Jannin, et al., Atypical human infections by animal trypanosomes, PLoS Neglected Trop. Dis. 7 (9) (2013), e2256.

[7] V.N. Van Chau, B.C. Le, M. Desquesnes, S. Herder, H.L.N. Phu, J.I. Campbell, et al., A clinical and epidemiological investigation of the first reported human infection with the zoonotic parasite Trypanosoma evansi in Southeast Asia, Clin. Infect. Dis. 62 (2016) 1002–1008.

[8] M.I. Takeet, S.O. Peters, B.O. Fagbemi, M. DeDonato, V.O. Takeet, M. Wheto, I. G. Imumorin Ig, Phylogeny of *Trypanosoma brucei* and *Trypanosoma evansi* in naturally infected cattle in Nigeria by analysis of repetitive and ribosomal DNA sequences, Trop. Anim. Health Prod. 48 (6) (2016) 1235–1240.

[9] M. Radwanska, N. Vereecke, V. Deleeuw, J. Pinto, S. Magez, Salivarian Trypanosomosis, A review of parasites involved, their global distribution and their interaction with the innate and adaptive mammalian host immune system, Front. Immunol. 2 (9) (2018), 02253.

[10] E.J. Dingwoke, F.A. Adamude, C.E. Chukwuocha, A.A. Ambi, N.N. Nwobodo, A. B. Sallau, H.C. Nzelibe, Inhibition of *Trypanosoma evansi* Protein-tyrosine phosphatase by Myristic acid analogues isolated from *Khaya senegalensis* and *Tamarindus indica*, J. Exp. Pharmacol. 11 (2019) 135–148.

[11] M. Desquesnes, P. Holzmuller, D. Lai, A. Dargantes, Z. Lun, S. Jittaplapong, *Trypanosoma evansi* and Surra: a review and perspectives on origin, history, distribution, taxonomy, morphology, hosts, and pathogenic effects, 2013, BioMed Res. Int. (2013) 1–22.

[12] G. Aregawi, G.E. Agga, R.D. Abdi, P. Buscher, Systematic review and meta- analysis on the global distribution, host range, and prevalence of Trypanosoma evansi, Parasites Vectors 12 (2019) 1–25.

[13] C.A. Hoare, The Trypanosomes of Mammals. A Zoological Monograph, Blackwell Scientific Publications, Oxford, 1972.

[14] E. Sánchez, T. Perrone, G. Recchimuzzi, I. Cardozo, N. Biteau, P.M. Aso, et al., Molecular characterization and classification of Trypanosoma spp. Venezuelan isolates based on microsatellite markers and kinetoplast maxicircle genes, Parasites Vectors 8 (2015) 536.

[15] M. Desquesnes, G. Bossard, S. Thévenon, D. Patrel, S. Ravel, D. Pavlovic, et al., Development and application of an antibody-ELISA to follow up a Trypanosoma evansi outbreak in a dromedary camel herd in France, Vet. Parasitol. 162 (2009) 214–220.

[16] A. Tamarit, C. Gutierrez, R. Arroyo, V. Jimenez, G. Zagalá, I. Bosch, et al., Trypanosoma evansi infection in mainland Spain, Vet. Parasitol. 167 (2010) 74–76.

[17] R.M. Powar, V.R. Shegokar, P.P. Joshi, V.S. Dani, N.S. Tankhiwale, O. Truc P, et al., A rare case of human trypanosomiasis caused by Trypanosoma evansi, Indian J. Med. Microbiol. 24 (2006) 72–74.

[18] N.P. Dakshinkar, R.M. Powar, V.R. Shegaokar, V.S. Dani, S.W. Kolte, W.A. Khan, Aberrant trypansomiasis in human, R Vet. J. India 3 (2007) 6–7.

[19] OIE (World Organization for Animal Health), OIE-Listed diseases, infections and infestations in force in 2018. http://www.oie.int/animal-health-inthe- world/oie-listed-diseases-2018/, 2018. (Accessed 18 March 2020). Accessed.

[20] P. Büscher, G. Cecchi, V. Jamonneau, G. Priotto, Human african trypanosomiasis, Lancet 390 (2017) 2397–2409.

[21] O. Diall, G. Cecchi, G. Wanda, R. Argilés-Herrero, M.J.B. Vreysen, G. Cattoli G, et al., Developing a progressive control pathway for African animal trypanosomosis, Trends Parasitol. 33 (2017) 499–509.

[22] H.R. Holt, R. Selby, C. Mumba, G.B. Napier, J. Guitian J, Assessment of animal African trypanosomiasis (AAT) vulnerability in cattle-owning communities of sub-saharan Africa, Parasites Vectors 9 (2016) 53–64.

[23] C. Cordon-Obras, P. Berzosa, N. Ndong-Mabale, L. Bobuakasi, J.N. Buatiche, P. Ndong-Asumu, Trypanosoma brucei gambiense in domestic livestock of Kogo and Mbini foci (Equatoria Guinea), Trop. Med. Int. Health 14 (5) (2009) 535–541.

[24] J. Singh, A.K. Upadhyay, A. Bahadur, Antioxidant phytochemicals in cabbage (*Brassica oleracea* L. var. capitata), Sci. Hortic. 108 (2006) 7–233.

[25] M. Wennberg, J. Ekvall, K. Olsson, Changes in carbohydrate and glucosinolate composition in white cabbage (*Brassica oleracea* var. capitata) during blanching and treatment with acetic acid, Food Chem. 95 (2006) 36–226.

[26] C.W. Beecher, Cancer preventive properties of varieties *of Brassica oleracea*: a review, Am. J. Clin. Nutr. 59 (1994) 1166–1170.

[27] G. Stoewsand, J. Anderson, L. Munson, Protective effects of dietary brussels sprouts against mammary carinogenesis in Sprague- Dawley Rats, Cancer Lett. 39 (1988) 199–207.

[28] E. Yurtsever, K.T. Yardimic, The *in vivo* effect of a *Brassica oleracea* var. capitata extract on Ehrlich ascites tumors of *Mus musculus* BALB/C mice, Drug Metabol. Drug Interact. 15 (2–3) (1999) 22–215.

[29] D. Samec, J. Piljac-Zegarac, M. Bogovi, Antioxidant potency of white (*Brassica oleracea* L. var. capitata) and Chinese (*Brassica rapa* L. var. pekinensis (Lour.) cabbage: the influence of development stage, cultivar choice and seed selection, Sci. Hortic. 128 (2011) 78–83.

[30] S.A. Chiplonkar, K.V. Tarwadi, R.B. Kavedia, Fortication of vegetarian diets for increasing bioavailable iron density using green leafy vegetables, Food Res. Int. 32 (1999) 169–174.

[31] C. Maritess, S. Small M. Waltz-Hill, Alternative nutrition therapies in cancer patients, Semin. Oncol. Nurs. 21 (2005) 6–173.

[32] A.C. Igweh, J.C. Aguiyi, F.K. Okwuasaba, Antitrypanosomal effect of the aqueous extract of *Brassica oleracea*, Fitoterapia 73 (2002) 17–21.

[33] P. Shaba, N.N. Pandey, O.P. Sharma, J.R. Rao, R.K. Antitrypanosomal, Effects of Brassica oleracea (cabbage) fruits and leaves, J. Vet. Adv. 2 (7) (2012) 304–401.

[34] H. Birhanu, R. Fikru, M. Said, W. Kidane, T. Gebrehiwot, A. Hagos, T. Alemu, T. Dawit, D. Berkvens, B.H. Goddeeris, P. Büscher, Epidemiology of Trypanosoma evansi and Trypanosoma vivax in domestic animals from selected districts of Tigray and Afar regions, Northern Ethiopia, Parasites Vectors 8 (212) (2015), https://doi.org/10.1186/s13071-015-0818-1.

[35] W.J. Herbert, W.H.R. Lumsden, Trypanosoma brucei: a rapid ''matching'' method for estimating the host's parasitemia, Exp. Parasitol. 40 (1976) 427–431.

[36] S.C.H. Ngomtcho, J.S. Weber, E.N. Bum, T.T. Gbem, S. Kelm, M.D. Achukwi, Molecular screening of tsetse flies and cattle reveal different *Trypanosoma* species including *T. grayi* and *T. theileri* in northern Cameroon, Parasites Vectors 10 (631) (2017) 1–16.

[37] E.R. Adams, I.I. Malele, A.R. Msangi, W. C. Gibson Trypanosome, Identification in wild tsetse populations in Tanzania using generic primers to amplify the ribosomal RNA ITS 1 region, Acta Trop. 100 (2006) 103–109.

[38] S. Kumar, G. Stecher, M. Li, C. Knyaz, K. Tamura, MEGA X: Molecular evolutionary genetics analysis across computing platforms, Mol. Biol. Evol. 35 (2018) 1547–1549.

[39] K. Tamura, M. Nei, Estimation of the number of nucleotide substitutions in the control region of mitochondrial DNA in humans and chimpanzees, Mol. Biol. Evol. 10 (1993) 512–526.

[40] D. Lorke, A new approach to acute toxicity testing, Arch. Toxicol. 54 (1983) 275.

[41] K.E. Ibrahim, M.G. Al-Mutary, A.O. Bakhiet, H.A. Khan, Histopathology of the liver, kidney, and spleen of mice exposed to gold nanoparticles, Molecules 23 (2018) 1848, 10.3390.

[42] A. Kaufer, J. Ellis, D. Stark, J. Barratt, The evolution of trypanosomatid taxonomy, Parasitol Vectors 10 (2017) 1–17.

[43] B.C. Weber, Extra vascular foci of *Trypanosoma vivaxin* goats: the central nervous system and aqueous humor of the eye as potential sources of relapse, J. Proteome Res. 13 (2009) 234–239.

[44] D. Biswas, A. Choudhury, K.K. Misra, Histopathology of *Trypanosoma* (Trypanozoon) *evansi* infection in bandicoot rat. II. Brain and choroid plexus, Proc. Zool. Soc. 63 (2010) 27–37.

[45] M.S. Bal, L.D. Singla, H. Kumar, A. Vasudev, K. Gupta, P.D. Juyal, Pathological studies on experimental *Trypanosoma evansi* infection in Swiss albino mice, J. Parasit. Dis. 36 (2) (2012) 260–264.

[46] M.A. Ghaffar, M. El-Melegy, A.F. Afifi, B.E.W. El-Aswad, N. El-Kady, A.F.I. Atia, The histopathological effects of *Trypanosoma evansi* on experimentally infected mice, Menoufia Med. J. 29 (4) (2016) 868–873.

[47] U. Frevert, A. Movila, O.V. Nokolskaia, J.R. Raper, Z.B. Mackey, M. Abdulla, J. Mckerrow, D.J. Grab, Early invasion of brain parenchyma by african trypanosomes, PLoS One 7 (8) (2012) 1–33.

[48] A. Aremu, E.I. Kingsley, B.K. Talha, A.O. Akeem, R.A. Ibrahim, A.G. Jimoh, K. Sulyman, S.K. Yusuf, Methanolic leaf extract of *Moringa oleifera* improves the survivability rate, weight gain and histopathological changes of Wister rats infected with *Trypanosoma brucei*, Intl. J. Vet. Sci. Med. 6 (2018) 30–44.

[49] M.D. Baldissera, C.F. Souza, C.M. Bertoncheli, K.L. Da Silveira, T.H. Grando, B.C. Z. Porto, D.B.R. LeaL, A.S. Da Silva, R.E. Mendes, L.M. Stefani, S.G. Monteiro, Oxidative stress in the heart of rats infected with *Trypanosoma evansi*, Kor. J. Parasitol. 54 (3) (2016) 247–252.

[50] P. Babokhov, A.O. Sanyaolu, W.A. Oyibo, A.F. Fagbenro-Beyioku, N.C. Iriemenam, A current analysis of chemotherapy strategies for the treatment of human African trypanosomiasis, Pathog. Glob. Health 107 (5) (2013) 242–252.

[51] Y.P. Nagagi, R.S. Silayo, C. Luziga, J. Eliningaya, E.J. Kweka, In vivo effect of *Commiphora swynnertonii* ethanolic extracts on *Trypanosoma congolense* and selected immunological components in mice, BMC Compl. Alternative Med. 17 (275) (2017) 1–14.

[52] V.O. Sekoni, Reproductive disorders caused by animal typanosomosis: a review, Theriogenology 42 (4) (1994) 557–570.